X-ray scattering studies of thin films of photosensitive polyimides

M. Ree* and T. L. Nunes
IBM Technology Products, Hopewell Junction, NY 12533, USA

and J. S. Lin
Solid State Division, Oak Ridge National Laboratory, Oak Ridge, TN 37831, USA
(Received 12 January 1993; revised 29 March 1993)

Using the techniques of wide-angle X-ray diffraction (WAXD) and small-angle X-ray scattering (SAXS), the morphology of polyimide thin films thermally imidized from several photosensitive polyimide (PSPI) precursors has been investigated and compared with that of the thin films prepared from the corresponding poly(amic acid) precursors: poly(4,4′-oxydiphenylene pyromellitimide) (PMDA-ODA), poly(*p*-phenylene biphenyltetracarboximide) (BPDA-PDA) and poly(4,4′-oxydiphenylene benzophenonetetracarboximide) (BTDA-ODA). The WAXD results indicate that regardless of the precursor origin, the BTDA-ODA polyimide is amorphous, whereas the other polyimides exhibit a molecular order. For both the PMDA-ODA and the BPDA-PDA, the molecular order is relatively higher in the films prepared from the PSPI precursors than in those from the corresponding poly(amic acid)s, indicating that during thermal imidization, the photosensitive groups play an important role to improve the mobility of the polymer chains, which may be critically needed to make better molecular packing, in spite of their bulkiness having the potential to hinder the molecular packing. In Lorentz-corrected SAXS analyses, a long period (130–156 Å mean periodicity) was observed for all the polyimides except the PMDA-ODA. In particular, the microstructure in the BPDA-PDA could be described by an extended chain-based two-phase (ordered and less ordered phase) model with diffuse boundaries because of its high chain rigidity. In addition, the Guinier SAXS analyses indicate the presence of voids in all the polyimide films, regardless of the precursor origin. The size of voids was 251–349 Å in radius, depending upon the type of polyimide.

(Keywords: polyimide; photosensitive polyimide; poly(amic acid))

INTRODUCTION

Photosensitive polyimides (PSPIs) have recently attracted great attention in the microelectronics industry because they are easily processable owing to their direct patternability, in addition to having excellent thermal stability, good mechanical properties and high chemical resistance[1–6]. Most PSPIs are based on polyimide precursors functionalized with a photochemically crosslinkable group (an acrylate or methacrylate derivative) through either ester bond (ester type) or acid/base complex (ionic type) formation. These PSPI precursors are generally formulated further with additives, such as photosensitizers and photoinitiators, to improve their photochemical performance in lithographic processes. For applications in the fabrication of microelectronic devices, these PSPI precursor solutions are cast in thin films, patterned by a lithographic process (photoexposure with a mask at either i-line, g-line or broad-band of a Hg lamp and developing with a solvent), and treated by a thermal imidization process. During thermal imidization, the photocrosslinkable groups are debonded from the polymer backbone by imide-ring closure, independent of the type of photochemical crosslinking, and outgassed from the resulting polyimide films.

Although the photocrosslinkable leaving groups are outgassed during thermal imidization, they may change the imidization kinetics of the precursors as well as the morphological structure in the condensed state, leading to different structures and properties in the resulting polyimides. The imidization kinetics of polyimide precursors has been studied by several research groups[7–9], using thermal gravimetry and thermal gravimetry/mass spectroscopy. For example, poly(4,4′-oxydiphenylene pyromellitamic acid) precursor exhibits the onset of imidization at ~130°C and its imidization is completed below 230°C[8]. Its ionic-type PSPI precursor with diethylaminoethyl methacrylate shows the onset of imidization at ~140°C, and the photosensitive groups outgas completely below 270°C[7,9]. On the other hand, the ester-type PSPI precursor with hydroxyethyl methacrylate exhibits the onset of imidization at 150°C and the outgas of the photosensitive groups still continues until 400°C[7,9]. Consequently, these results indicate that the imidization kinetics of a polyimide precursor depends strongly on the precursor type as well as the functional leaving group. Recently, Ree *et al.*[10,11] have reported that the residual stress and mechanical properties of thermally imidized PSPI films are quite different from those of the corresponding polyimide films prepared from the

* To whom correspondence should be addressed at: Pohang Institute of Science and Technology, Department of Chemistry, PO Box 125, Pohang, Kyongbuk 790-600, South Korea

0032-3861/94/06/1148–09

poly(amic acid) precursors, indicative of the significant influence of the photocrosslinkable groups. The difference between the properties of a PSPI and its conventional polyimide was strongly dependent on the polymer chain rigidity: the higher chain rigidity gave the larger difference in the properties. Thus, the effect of the photosensitive group on final film properties is very significant in rigid-type polyimides, such as poly(*p*-phenylene pyromellitimide) (PMDA-PDA) and poly(*p*-phenylene biphenyltetracarboximide) (BPDA-PDA).

Sometimes, it may be difficult to completely outgas photocrosslinkable groups (particularly for ester-type PSPIs) as well as additives (photosensitizers and photoinitiators) from resulting polyimide films, depending upon their boiling point and thermal degradation temperature as well as imidization temperature. If they do not outgas completely, they may remain in the films as residues and, consequently, affect final film properties. Also, microcavities may be generated in the resulting polyimide films by outgassing of relatively bulky photosensitive groups during thermal imidization.

Ionic-type PSPI precursors without additives may be ideal for studying the influence of photosensitive groups on the morphology of resulting polyimides because of their easier removal during thermal imidization. For this reason, several ionic-type PSPI precursors with various chain rigidities were prepared in the present study as model PSPI systems in order to investigate the effect of photosensitive groups on final film morphology: PMDA-ODA, BPDA-PDA and poly(4,4′-oxydiphenylene benzophenonetetracarboximide) (BTDA-ODA) PSPI precursors (see *Figure 1*). The morphology (i.e. molecular order, microstructure and microvoids) of thin polyimide films thermally imidized from these PSPI precursors was investigated by small-angle X-ray scattering (SAXS) and wide-angle X-ray diffraction (WAXD), and compared with that of the films prepared from the corresponding poly(amic acid)s.

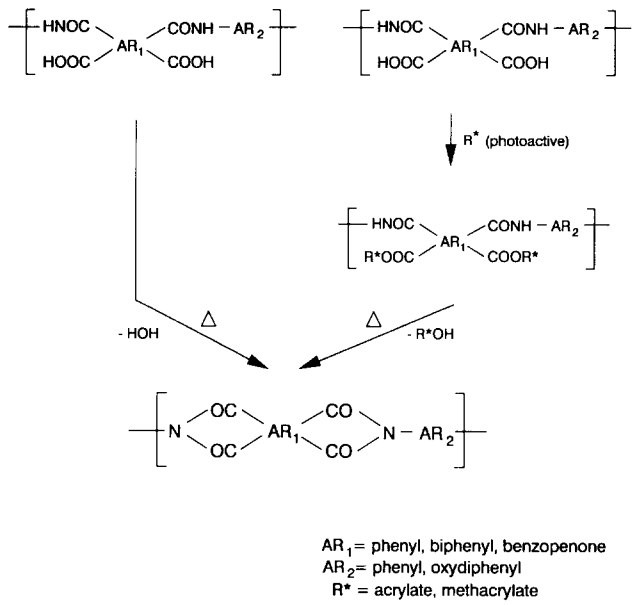

Figure 1 Polyimide formations from poly(amic acid) precursors and photosensitive polyimide precursors

EXPERIMENTAL

Materials and film preparation

Poly(4,4′-oxydiphenylene pyromellitamic acid) (PMDA-ODA PAA) ($\bar{M}_w \sim 35 \times 10^3$ and 16.0 wt%) precursor and poly(*p*-phenylene biphenyltetracarboxamic acid) (BPDA-PDA PAA) ($\bar{M}_w \sim 40 \times 10^3$ and 13.5 wt%) solutions were obtained from Du Pont Chemical Company. Poly(4,4′-oxydiphenylene benzophenonetetracarboxamic acid) (BTDA-ODA PAA) ($\bar{M}_w \sim 40 \times 10^3$ and 18.0 wt%) precursor solution was prepared in *N*-methyl-2-pyrrolidone (NMP) through polymerization from the respective dianhydride and diamine purified through sublimation. The photosensitive precursor solutions of these poly(amic acid) precursors were prepared by attaching a photocrosslinkable monomer, 2-(dimethylamino)ethyl methacrylate (DMAEM; Aldrich Chemical Co.) to the carboxylic acid groups of the precursors through acid/amine ionic complexation. Then, DMAEM of 100 mol% stoichiometry (to the carboxylic groups) was added to each precursor solution in a known amount and mixed at room temperature for 1 day, using a roller mixer. In addition, a commercial photosensitive polyimide precursor formulation, Photoneece UR-3840, was received from Toray Chemical Co. Photoneece UR-3840 is known to be a PSPI based on BTDA-ODA PAA ionically complexed with a methacrylate[12]. All the precursor solutions were stored in a refrigerator. The refrigerated solutions were held at room temperature for ~5 h before use.

All the polyimide precursor solutions were spin-coated on silicon wafers cleaned in an O_2 plasma asher and softbaked at 80°C for 30 min in a convection oven with a nitrogen flow. The softbaked samples were thermally imidized in a Heraeus oven with a nitrogen flow by a step-cure process: 150°C/30 min, 230°C/30 min, 300°C/30 min and 400°C/1 h. The ramping rate for each step was 2.0 K min^{-1} and the cooling rate was 1.0 K min^{-1}. The thickness of cured films was ~10 μm.

Measurements

WAXD patterns were collected from the single polyimide films on a Rigaku CN2155 powder diffractometer. The diffractometer was mounted in a vacuum tank to reduce air scatter of the β-filtered Cr Kα radiation. The X-ray generator was run at 35 kV and 40 mA. One-half degree defining and scatter slits were used together with a 0.3 mm receiving slit. Step and count data were taken under computer control at 0.1° (2θ) intervals with a counting time of 8–60 s per step, depending upon whether a transmission or reflection scan was being made. Diffractograms were collected with the diffraction vector both normal to and in the plane of the polyimide films. All WAXD measurements were performed in $\theta/2\theta$ mode.

Coherence lengths and percentage crystallinities were estimated from WAXD patterns corrected to the background runs in the following manner. An interactive curve-fitting technique based on Marquardt's non-linear least-squares estimation algorithm[13] was used to fit a collection of Gaussian functions and one linear baseline to the raw data. Coherence lengths (L_C) were estimated from the Scherrer relationship[14,15]:

$$L_C = \frac{\lambda}{FWHM \cos\theta} \quad (1)$$

where λ is the wavelength of the X-ray radiation source and $FWHM$ is the full width at half maximum of the

Gaussian fit to the X-ray reflection peak in radians, corrected for an instrument broadening of 0.15° (2θ).

The percentage crystallinity was estimated by dividing the area under all of the Gaussian functions fit to crystalline peaks by the total area of all Gaussian functions required to fit the diffractogram. For the films which show anisotropy, it is noted that the percentage crystallinity calculated in this way is not a true bulk crystallinity, but an effective crystallinity associated only with the direction of the diffraction vector either in the film plane or normal to it.

For measurements of small-angle X-ray scattering (SAXS), the polyimide films removed from the wafers were diced to a dimension of 20 mm × 20 mm using a blade. The diced film pieces were stacked together to a total thickness of ~150 μm. For the multistacked films, SAXS measurements were performed in a configuration with the scattering vector parallel to the film plane. The SAXS measurements were conducted using the ORNL 10 m SAXS system with a pinhole (1 mm^2) collimator and a pyrolytic graphite-monochromatized Cu Kα radiation source operated at 40 kV and 50 mA. The sample-to-detector distances used were 1.620 m ($0.1411 \leqslant q \leqslant 3.1494\ \text{nm}^{-1}$) and 5.126 m ($0.0652 \leqslant q \leqslant 1.0615\ \text{nm}^{-1}$), where $q=(4\pi/\lambda)\sin\theta$ with the wavelength (λ) of a radiation source and scattering angle (2θ). A 64 × 64 array two-dimensional position-sensitive detector was attached to an on-line display system. In SAXS measurements, it is generally necessary to perform additional measurements for the background run (that is, empty beam run), the dark current run, and the detector sensitivity run using a radioactive isotope ^{55}Fe, beside a sample run, because of the unavoidable contributions of the detectable counts from cosmic radiation, parasitic scattering from collimation slits or pinholes, and possible non-uniform efficiency of the detector. The measurement of sample transmission for the primary X-ray beam is also needed to correct for beam absorption by samples. All the measurements were carried out according to the standard procedure of the CSASR (Center for Small Angle Scattering Research) at Oak Ridge National Laboratory[16]. The two-dimensional SAXS intensities measured were corrected for all the unavoidable contributions and sample absorption. The corrected SAXS patterns were isotropic, and their two-dimensional intensities were averaged circularly.

The circularly averaged SAXS intensity profiles were Lorentz-corrected, and plotted with the magnitude of scattering vector q. The mean periodicity revealing a microstructure in films was estimated from the peak maximum in the Lorentz-corrected SAXS intensity profiles. The voids in films are also of interest in the present study. The SAXS arising from voids was analysed by the Guinier law[17,18]:

$$I(q)=I(0)\exp\left(\frac{-q^2R_g^2}{3}\right) \qquad (2)$$

where $I(q)$ is the scattered intensity at a scattering vector $\mathbf{q}$, $I(0)$ is the scattered intensity at zero angle, and R_g is the radius of gyration of the particles. Therefore, the average size of the scatterers is determined from the plot of $\ln I(q)$ *versus* q^2.

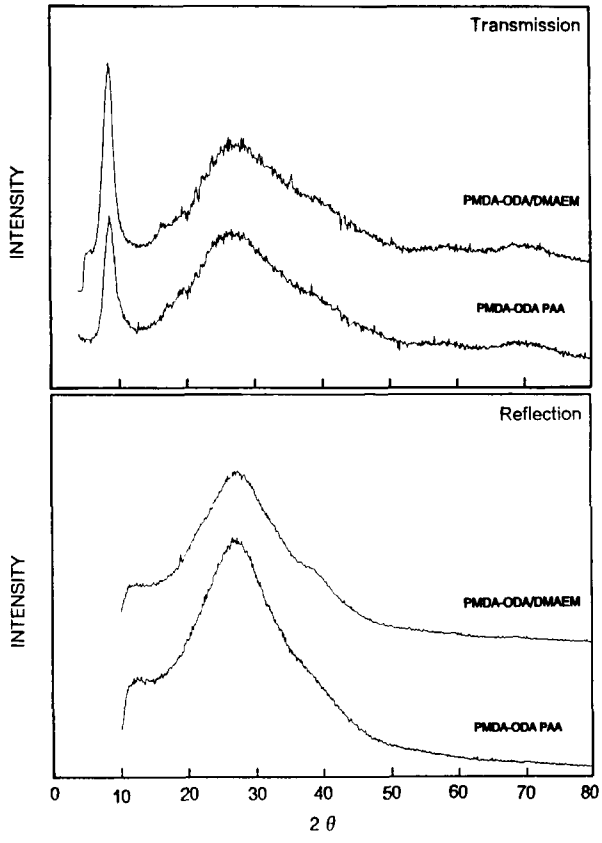

Figure 2 WAXD transmission and reflection patterns of the PMDA-ODA polyimide films prepared thermally from both PMDA-ODA PAA and PMDA-ODA/DMAEM precursors. Cr Kα radiation was used. The film thickness was ~10 μm

RESULTS AND DISCUSSION

Semiflexible PMDA-ODA polyimide

Figure 2 shows the WAXD patterns from the PMDA-ODA polyimide thin films imidized thermally from both conventional PMDA-ODA PAA and photosensitive PMDA-ODA/DMAEM precursors. The transmission WAXD patterns exhibit a single sharp peak in a low-angle region of $2\theta < 12°$ and several broad peaks in a high-angle region of $2\theta > 12°$. The broad peak over $12° < 2\theta < 50°$ may correspond to the diffraction of a poor intermolecular packing combined with the amorphous halo. From the maximum of the broad peak, the mean intermolecular distance is 4.9 Å (27.04° 2θ) for the polyimide film from the PMDA-ODA PAA and 4.8 Å (27.61° 2θ) for the corresponding film from the PMDA-ODA/DMAEM. That is, the polymer molecules are more densely packed in the film from the PSPI precursor than in the film from the poly(amic acid). The very weak, broad peaks over the range of $35° < 2\theta < 80°$ may result from an intramolecular chain order and a poor intermolecular packing order, as previously described by Takahashi *et al.*[19] and Yoon *et al.*[20]. The single sharp diffraction peak at 8.47° (2θ) has a d-spacing of 15.5 Å, corresponding to the projected length of the chemical repeat unit ordered along the chain axis. The coherence length (L_C) for this peak is 74 Å (corresponding to four to five chemical repeat units) for the PMDA-ODA PAA and 85 Å (corresponding to five to six chemical repeat units) for the PMDA-ODA/DMAEM. Consequently, molecular chain order (along the chain axis) is slightly higher in the polyimide film prepared from the PMDA-ODA/DMAEM than in the corresponding film from the PMDA-ODA PAA. This sharp peak in the low-angle region is not observed in the

reflection patterns with the diffraction vector normal to the film plane, regardless of the precursor origin. This indicates that the PMDA-ODA molecules are highly oriented in the film plane, regardless of the precursor origin. In addition, the crystallinity estimated from the transmission WAXD pattern was 12.5% for the PMDA-ODA PAA and 16.8% for the PMDA-ODA/DMAEM. Overall, the molecular order in the PMDA-ODA polyimide film was enhanced by the photosensitive groups linked to the poly(amic acid) precursor.

In general, softbaked PMDA-ODA PAA films exhibit two distinct peaks on both reflection and transmission WAXD patterns[19,20]. The first peak in a low-angle region is relatively sharp and appears at a d-spacing of ~ 14.4 Å, corresponding to the projected length of the chemical repeat unit along the chain axis. The second broad peak with a mean d-spacing of ~ 4.9 Å is the amorphous halo. The PMDA-ODA PAA film in the condensed state is known to have a liquid-crystal-like chain order with a lack of intermolecular packing order[19]. The photosensitive DMAEM group is relatively bulky in comparison with the hydrogen of carboxylic acid groups in the PMDA-ODA PAA precursor. Thus, the structure of the PMDA-ODA PAA film in the condensed state may be disturbed by attaching the bulky photosensitive groups to the precursor backbone. However, the WAXD patterns of PMDA-ODA/DMAEM films, which were softbaked at 80°C, are very similar to those of the PMDA-ODA PAA films[21], indicating no significant effect of the bulky photosensitive group on the molecular order in the softbaked precursor film.

During imidization, the bulky DMAEM groups may play two different roles. First, the bulky groups may hinder the formation of extended chains of the precursor molecules being imidized, leading to less chain and packing orders in resulting polyimide films. Second, the DMAEM monomer is a liquid with a boiling point of 182–192°C and hence, the attached DMAEM groups lower the glass transition temperature (T_g) of the PMDA-ODA PAA films, resulting in an increase in the chain mobility. Furthermore, the DMAEM groups, which are detached from the backbone by imide-ring closure during thermal imidization, may behave as plasticizers until outgassed. This also increases the chain mobility of the precursors being imidized as well as of the resulting polyimide molecules. These enhanced molecular chain mobilities may lead to better molecular order and higher crystallinity. As described above, the WAXD results indicate that in spite of the bulkiness of DMAEM, the polyimide film prepared from the PSPI precursor exhibits higher molecular order than that from the PMDA-ODA PAA. Therefore, the better molecular order and higher crystallinity in the films from the PSPI precursor might result from the increased mobility of the polymer chains provided by the photosensitive DMAEM groups during thermal imidization.

For the polyimide films, SAXS measurements were performed over $0.0652 \leqslant q \leqslant 3.1494\ \mathrm{nm}^{-1}$. Some results are shown in *Figure 3*. The PMDA-ODA polyimide films did not exhibit any SAXS peak on either the scattered intensity or the Lorentz-corrected scattered intensity plots with the magnitude of scattering vector q, regardless of the precursor origin. This result indicates that no microstructure has been developed in the PMDA-ODA polyimide films thermally imidized from both the precursors.

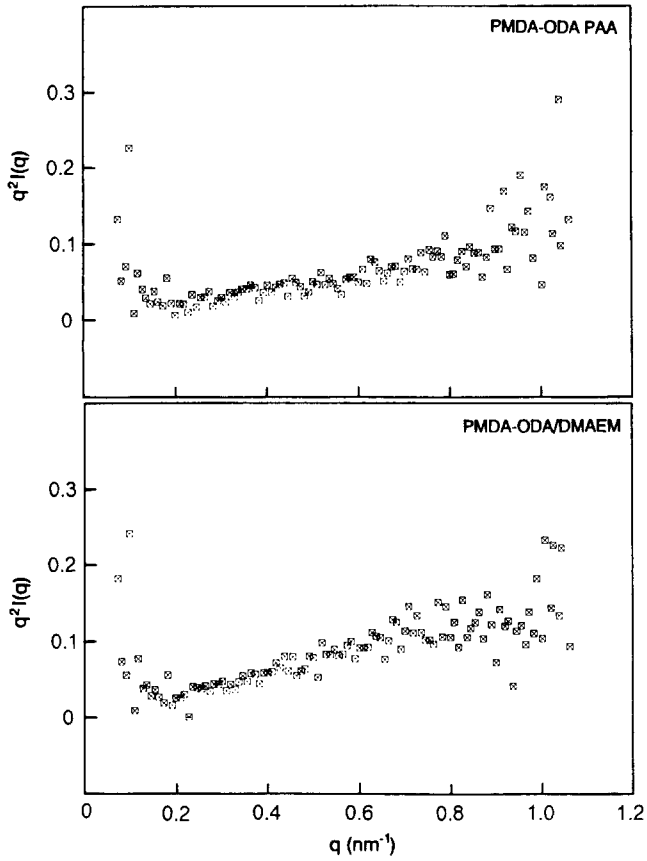

Figure 3 Lorentz-corrected SAXS profiles of the PMDA-ODA polyimide films prepared thermally from both PMDA-ODA PAA and PMDA-ODA/DMAEM precursors. Cu Kα radiation was used

In the case of the poly(amic acid), the SAXS result is quite different from the results previously reported elsewhere[22,23]. In the SAXS study of Isoda *et al.*[22], neither dried PMDA-ODA PAA films nor their resulting polyimide films imidized on substrates at a low temperature (100°C/3.5 h, 160°C/8 h, 200°C/4 h and 250°C/5.5 h) showed any peak on the SAXS curves, whereas only the polyimide films imidized on substrates above 280°C exhibited a single peak. This temperature (280°C) seems to be a critical curing temperature to form a microstructure in PMDA-ODA. The thickness of the polyimide films used was not reported. The authors concluded that the molecular aggregation is an amorphous structure in the dried PMDA-ODA PAA films and the polyimide films imidized at a low temperature (below 250°C), but is a two-phase structure in the polyimide films imidized above 280°C. The proposed two-phase structure, which can be explained in terms of a one-dimensional model, consists of segmental aggregates arranged periodically in space. Here, the polyimide chain segments are oriented perpendicularly to the direction of periodicity. In contrast, Russell[23] has observed a single peak indicating a periodicity of molecular aggregations on the SAXS curves for the polyimide films imidized even below 280°C, as well as the precursor films dried at 79°C or 100°C. In comparison, our polyimide samples were prepared differently in the following two aspects. First, the polyimide films were imidized on substrates by a step-cure process (150°C/30 min, 230°C/30 min, 300°C/30 min and 400°C/1 h). Second, the polyimide films were relatively very thin, $\sim 10\ \mu$m. According to the SAXS results of both

Isoda *et al.* and Russell, our PMDA-ODA polyimide film is expected to have a microstructure. However, our SAXS result for the thin polyimide films has not shown any peak and is therefore not consistent with their results. Therefore, one can speculate that the development of a microstructure in PMDA-ODA polyimide films is dependent upon the film thickness. Consequently, there is still an open question about the effects of the imidization process, substrate (that is, substrate-induced in-plane orientation of molecules) and film thickness on the development of a microstructure in thermally imidized PMDA-ODA.

In addition, the SAXS from voids in the PMDA-ODA polyimide films has been studied using the Guinier analysis[17,18]. The Guinier plots of the SAXS data are shown in *Figure 4*. The Guinier analyses indicate that the size of voids being presented in the polyimide films is ~ 260 Å in radius (R_g), regardless of the precursor origin. Similar results have been previously reported for the PMDA-ODA film thermally cured from the poly(amic acid)[24]: voids of $R_g = 50$–100 Å and volume fraction of 7×10^{-4}.

Semirigid BPDA-PDA polyimide

The morphological structure of thermally cured BPDA-PDA polyimide has been previously investigated in detail by WAXD measurements and structural refinement analysis[20,25]. The conclusion is that the BPDA-PDA polyimide molecules in films are in a frozen smectic-E crystalline state, exhibiting high molecular packing order with extended chains.

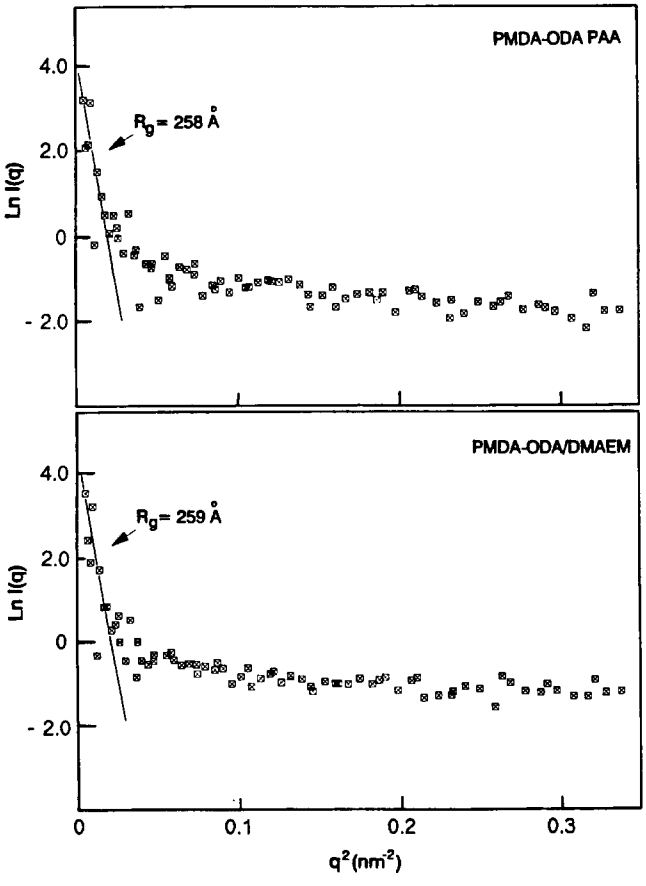

Figure 4 Guinier plots of the SAXS profiles of the PMDA-ODA polyimide films prepared thermally from both PMDA-ODA PAA and PMDA-ODA/DMAEM precursors. Cu Kα radiation was used

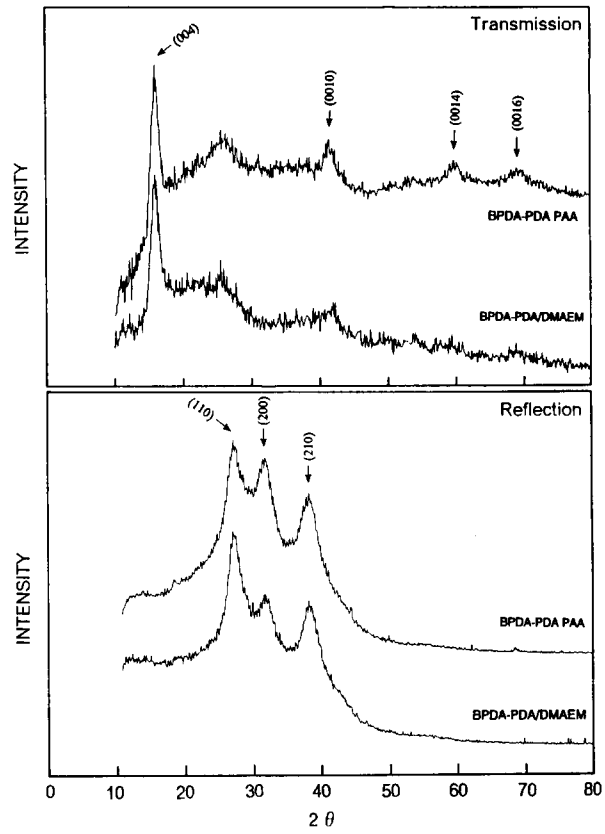

Figure 5 WAXD transmission and reflection patterns of the BPDA-PDA polyimide films prepared thermally from both BPDA-PDA PAA and BPDA-PDA/DMAEM precursors. Cr Kα radiation was used. The film thickness was $\sim 10\ \mu$m

In the present study, BPDA-PDA polyimide thin films of $\sim 10\ \mu$m thick were thermally prepared from both BPDA-PDA PAA and BPDA-PDA/DMAEM precursors. Their WAXD patterns are shown in *Figure 5*. The transmission WAXD patterns show mainly (0 0 *l*) peaks, such as (0 0 4), (0 0 10), (0 0 14) and (0 0 16). This result indicates that in the transmission geometry the scattering vector, which is in the film plane, coincides with the direction of the preferred orientation of the polyimide chains, that is, the polymer molecules are highly aligned in the film plane. The (0 0 4) peak for the film cured from the BPDA-PDA PAA is apparently identical with that for the film from the PSPI precursor in both peak intensity and width. Regardless of the precursor origin, the L_C for the (0 0 4) peak at 16.69° (2θ) is 104 Å, corresponding to six to seven chemical repeat units with the projected repeat unit length of 15.8 Å. However, the higher order (0 0 *l*) peaks were significantly affected by the photosensitive DMAEM groups, that is, the (0 0 10) peak became weak in intensity and broad in shape, and (0 0 14) and (0 0 16) peaks almost disappeared.

BPDA-PDA polyimide chains have a kink type of conformation per chemical repeat unit due to the bond between phenyl groups of the BPDA unit. According to a previous structural analysis[25], the two phenyl groups are coplanar. Thus, the polyimide may have *cis*, *trans* conformation, or mixed conformation via chain rotations along the kink bond, that is, there is a strong possibility of rotational disorder on the polymer chains owing to the conformational changes. The chain conformation may be very sensitive to the precursor origin as well as to the history of the polyimide film process. Any change

in the chain conformation may vary the direction of chains, consequently affecting the intermolecular packing order. However, the overall chain order along the chain axis is independent of the rotational disorder because of its extended chain characteristics. The L_C of the (0 0 4) peak in the transmission indicates that the crystalline order along the chain axis is not degraded by the photosensitive groups. Furthermore, the intermolecular packing order was enhanced by the photosensitive group: this is discussed in further detail below. Therefore, in the transmission WAXD pattern the weakening of the higher order (0 0 l) peaks because of the photosensitive groups might be caused by the change of molecular in-plane orientation rather than the degradation of molecular chain order. The birefringence ($\Delta = n_{xy} - n_z$), which was estimated from the in-plane (n_{xy}) and out-plane (n_z) refractive indices measured at 632.8 nm, is 0.240 for the polyimide film from the BPDA-PDA PAA and 0.1961 for the film from the PSPI precursor, indicative of a significant degradation of the chain in-plane orientation by the photosensitive groups[21].

The reflection WAXD pattern was also influenced by the photosensitive groups. The BPDA-PDA films showed three major peaks, regardless of the precursor origin: (1 1 0) at 27.20° (4.9 Å), (2 0 0) at 31.65° (4.2 Å), and (2 1 0) at 38.30° (3.4 Å). The (1 1 0) peak intensity was apparently increased by the photosensitive groups, whereas the (2 0 0) peak intensity was decreased. However, the (2 1 0) peak was apparently unchanged in shape. For the film from the BPDA-PDA PAA, coherence length was 69 Å for the (1 1 0) peak, 74 Å for (2 0 0) and 48 Å for (2 1 0). On the other hand, for the film from the PSPI precursor coherence length was 70 Å for the (1 1 0) peak, 88 Å for (2 0 0) and 59 Å for (2 1 0). Overall, the coherence lengths for the (h k 0) peaks were slightly enhanced by the photosensitive DMAEM groups linked to the precursor, indicative of an increase in the intermolecular packing order in the resulting polyimide film.

The overall crystallinity in the polyimide films was estimated from both the transmission and reflection WAXD patterns. The overall crystallinity estimated from the transmission pattern was 25% for the polyimide film from the BPDA-PDA PAA. It is noted here that this crystallinity is not a true crystallinity because of the high contribution from the (0 0 l) peaks. In comparison with the polyimide film from the BPDA-PDA PAA, the corresponding polyimide film from the PSPI precursor is expected to have a crystallinity less than 25% because of relatively less contribution from the (0 0 l) peaks. However, the lateral crystallinity, which was estimated from the reflection pattern, was 18% for the BPDA-PDA polyimide from the BPDA-PDA PAA and 24% for the corresponding polyimide film from the PSPI precursor.

It has been conclusively shown that in BPDA-PDA polyimide films the molecular packing order and overall crystallinity were improved by the photosensitive DMAEM groups. This might result from the improvement in chain mobility by the photosensitive groups during thermal imidization, as discussed earlier for the PMDA-ODA PSPI. During thermal imidization, the increased chain mobility provided by the photosensitive groups, through lowering of T_g and plasticizing, might counter their hindering of molecular packing due to their bulkiness and overcome it, finally leading to a better packing order in the resulting polyimide films. This suggests that in high T_g polyimides such as PMDA-ODA and BPDA-PDA, during imidization a high degree of chain mobility is necessary to form a better molecular order in the resulting polyimides.

Figure 6 shows the Lorentz-corrected SAXS profiles for the polyimide films. They show a single distinct peak maximum over $0.0735 \leqslant q \leqslant 1.0615\ \mathrm{nm}^{-1}$. The peak is broader for BPDA-PDA PAA than for BPDA-PDA/DMAEM. In the SAXS measurements, the incident X-ray beam was normal to the film plane and, therefore, the scattering vector was in the film plane. Thus, this SAXS measurement can provide morphological information on microstructures in the film plane. In fact, a microstructure in the film plane is expected to be different from that in the direction normal to the film plane, because of the high in-plane orientation of the polyimide molecules (see *Figure 5*). The mean periodicity was 156 Å for the polyimide film from the BPDA-PDA PAA and 142 Å for the film from the PSPI precursor. According to the WAXD results described above, the coherence length was 104 Å along the chain axis (i.e. L_C for (0 0 4)) and 48–88 Å in the lateral direction. Therefore, based on the periodicities (142 Å and 156 Å) with these crystalline sizes, it is possible that the long periodicity is either along the chain axis, in the lateral direction or in both directions. As illustrated in *Figure 6*, in the Lorentz-corrected SAXS plots for both the polyimide films the single peak is relatively broad compared with a typical SAXS peak from the folded lamellae in a linear polyethylene[26]. This suggests that the long periodicity is in the chain axis as well as the lateral direction. A detailed analysis of this matter is in progress. The BPDA-PDA

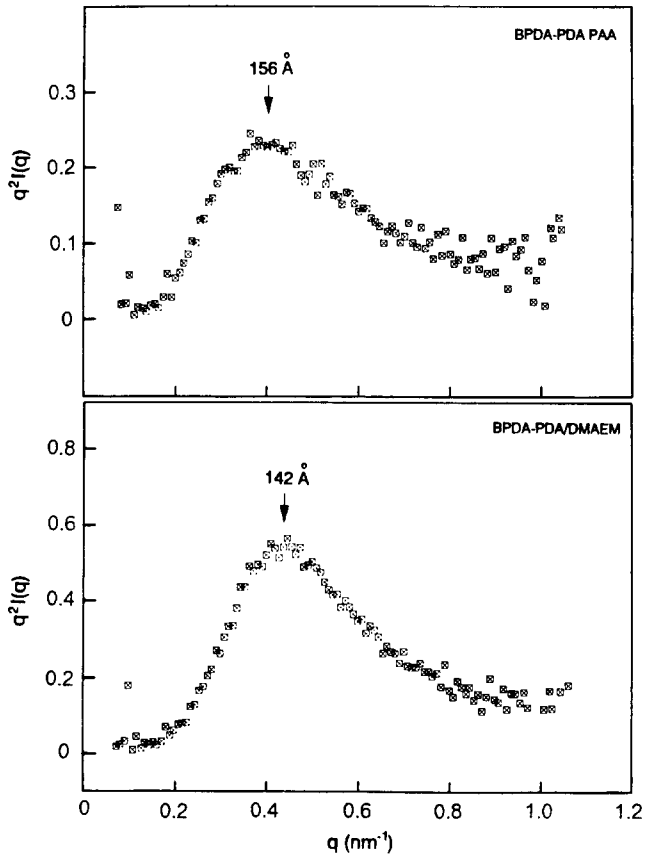

Figure 6 Lorentz-corrected SAXS profiles of the BPDA-PDA polyimide films prepared thermally from both BPDA-PDA PAA and BPDA-PDA/DMAEM precursors. Cu Kα radiation was used

polyimide chain is relatively rigid and its Kuhn segment length[27,28] is ~104 Å. Thus, its crystalline components consist of extended chains rather than folded chains. In addition to this, the phase boundaries between ordered and less ordered phases are expected to be very diffuse rather than sharp. This may also contribute to broadening the SAXS peak. The morphological microstructure in the BPDA-PDA polyimide films can be described by a two-phase model having diffuse boundaries with Hosemann's paracrystalline lattice statistics[29].

Figure 7 shows the Guinier plots of the SAXS data for the polyimide films from both the precursors. Voids were also observed in the BPDA-PDA polyimide films, regardless of the precursor origin. The average size of voids was ~334 Å in radius for BPDA-PDA PAA and ~349 Å for BPDA-PDA/DMAEM. These voids are slightly larger than those observed in the PMDA-ODA polyimides (see *Figure 4*).

Flexible BTDA-ODA polyimide

The WAXD results for the polyimide films from both BTDA-ODA PAA and its PSPI precursor (Photoneece UR-3840) are illustrated in *Figure 8*. The polyimides exhibited only featureless amorphous haloes in both reflection and transmission patterns, regardless of the precursor origin. For the first-order amorphous halo peaks, the mean intermolecular distance is 4.9 Å. In comparison, the halo peak ($10° < 2\theta < 55°$) from BTDA-ODA PAA was slightly stronger in intensity and sharper

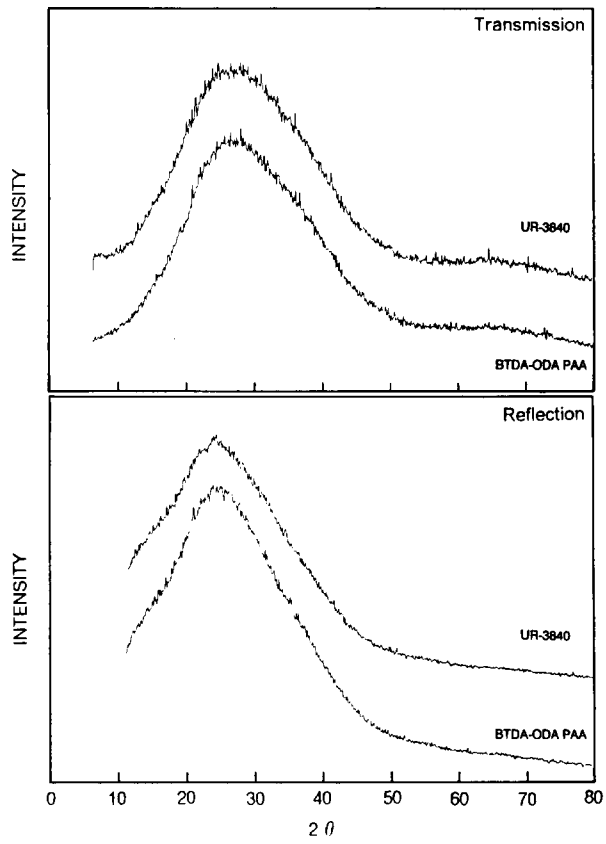

Figure 8 WAXD transmission and reflection patterns of the BTDA-ODA polyimide films prepared thermally from both BTDA-ODA PAA precursor and UR-3840 PSPI formulation. Cr Kα radiation was used. The film thickness was ~10 μm

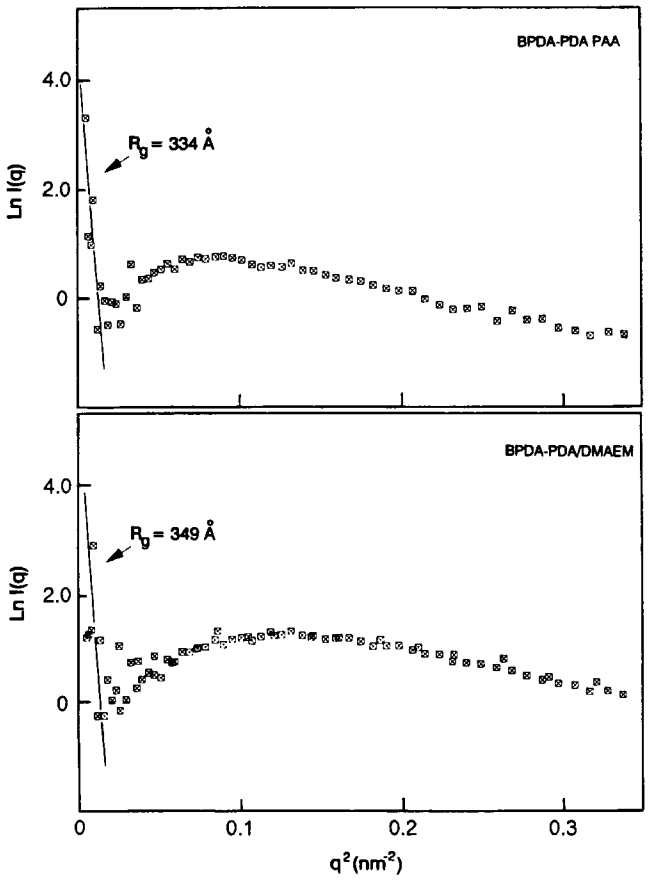

Figure 7 Guinier plots of the SAXS profiles of the BPDA-PDA polyimide films prepared thermally from both BPDA-PDA PAA and BPDA-PDA/DMAEM precursors. Cu Kα radiation was used

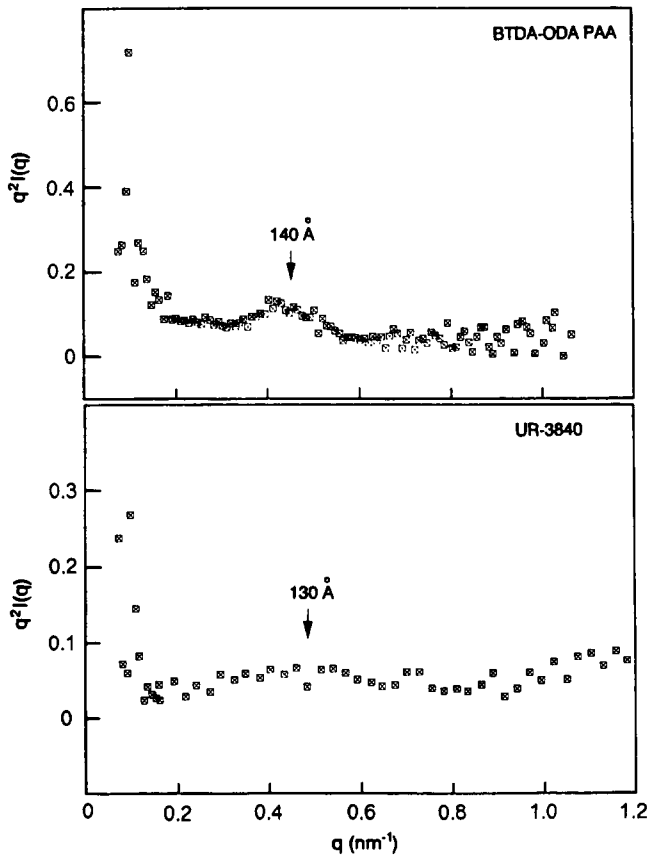

Figure 9 Lorentz-corrected SAXS profiles of the BTDA-ODA polyimide films prepared thermally from both BTDA-ODA PAA precursor and UR-3840 PSPI formulation. Cu Kα radiation was used

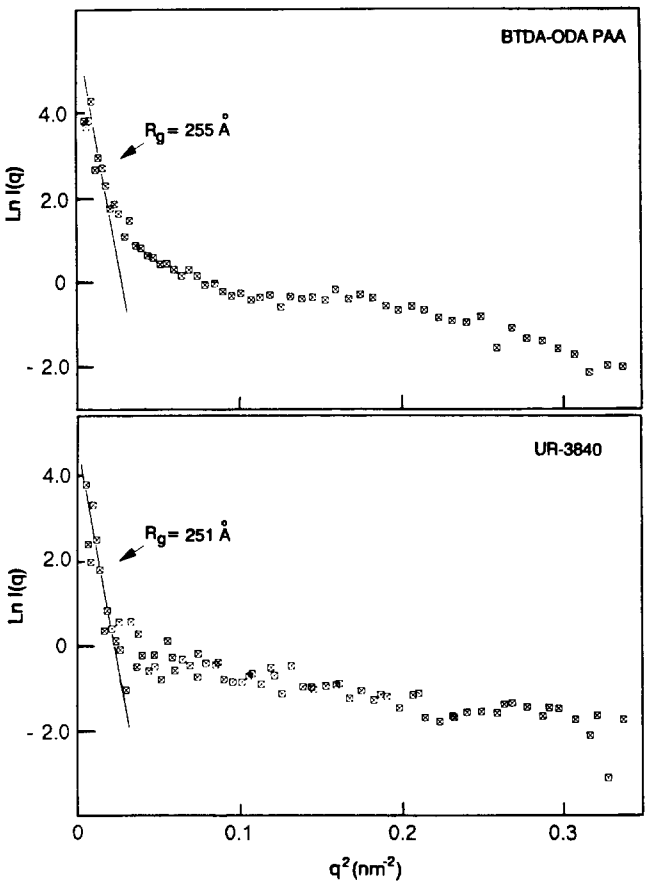

Figure 10 Guinier plots of the SAXS profiles of the BTDA-ODA polyimide films prepared thermally from both BTDA-ODA PAA precursor and UR-3840 PSPI formulation. Cu Kα radiation was used. R_g, radius of gyration

in shape than that from UR-3840. Except for this, no difference was detected in the WAXD patterns of the two polyimide films.

Figures 9 and *10* show the Lorentz-corrected plots and the Guinier plots of the SAXS intensity profiles from both the polyimide films, respectively. In the Lorentz-corrected SAXS plots, a very weak, broad peak was detected for both the polyimide films. The mean long period was 140 Å for the BTDA-ODA PAA and 130 Å for the UR-3840. The results indicate that a microstructure in a two-phase system has developed poorly in the BTDA-ODA polyimide films: the difference between electron densities of ordered and less ordered phases is small and the population of the ordered phase is also low. As observed in both PMDA-ODA and BPDA-PDA polyimides, voids were detected in the BTDA-ODA films. The average radius of the voids was ~253 Å.

CONCLUSIONS

The morphology (molecular order, microstructure and microvoids) of thin films of several polyimides, which were prepared thermally from their photosensitive precursors as well as conventional poly(amic acid) precursors, was investigated by WAXD and SAXS analyses. The WAXD results indicate that both semiflexible PMDA-ODA and semirigid BPDA-PDA polyimides are in a partially ordered state, regardless of the precursor origin, whereas fully flexible BTDA-ODA polyimide is in an amorphous state. Both the PMDA-ODA and the BPDA-PDA polyimides in thin films are highly oriented in the film plane. For these two polyimides, the molecular order and overall crystallinity are improved by the photosensitive DMAEM group in spite of its bulkiness which may hinder the molecular ordering. These indicate that during imidization the enhanced mobility of chains being provided by the photosensitive groups, which plasticize the imidizing precursor and lower its T_g, is critical, particularly in structural forming of high T_g polyimides such as semirigid BPDA-PDA and semiflexible PMDA-ODA.

In Lorentz-corrected SAXS analyses, the PMDA-ODA polyimides did not reveal any periodicity, whereas, regardless of the precursor origin, the other polyimides exhibited a long period of 130–160 Å (mean periodicity), depending upon the type of polyimide. However, the mean periodicity was slightly larger in the polyimides from the poly(amic acid) precursors than in the corresponding polyimides from the photosensitive precursors. The microstructures could be described by an extended chain-based two-phase (ordered and less ordered phase) model with diffuse boundaries. The Guinier SAXS analyses indicate the presence of voids in all the polyimide films studied here, independent of the precursor origin; these are 251–349 Å in radius, depending on the type of polyimide. However, in a study of water sorptions for these polyimide films[10,11], despite the enhanced molecular order and crystallinity the polyimide films prepared from the PSPI precursors exhibit a relatively higher water uptake and diffusion coefficient than those from the corresponding poly(amic acid)s. This suggests that another family of voids with $R_g > 350$ Å is present, with a relatively higher population in the polyimide films from the PSPI precursors.

REFERENCES

1 Rubner, R., Ahne, H., Kuhn, E. and Kolodziej, G. *Photogr. Sci. Eng.* 1979, **23**, 303
2 Yoda, N. and Hiramoto, H. *J. Macromol. Sci.-Chem.* 1984, **A21**, 1641 and references therein
3 Merrem, H. J., Klug, R. and Hartner, H. in 'Polyimides: Synthesis, Characterization, and Applications', (Ed. K. L. Mittal), Plenum, New York, 1984, p. 919
4 Pfeifer, J. and Rohde, O. in 'Recent Advances in Polyimide Science and Technology', (Eds W. D. Weber and M. R. Gupta), Plenum, New York, 1985, p. 336
5 Khanna, D. N. and Mueller, W. H. *Polym. Eng. Sci.* 1989, **29**, 954
6 Kubota, S., Yamawaki, Y., Moriwaki, T. and Eto, S. *Polym. Eng. Sci.* 1989, **29**, 950
7 Hiramoto, H. *Mater. Res. Soc. Symp. Proc.* 1989, **167**, 87
8 Volksen, W. *et al.* unpublished results
9 Chace, M. *et al.* unpublished results
10 Ree, M., Nunes, T. L., Chen, K. J. and Czornyj, G. *Mater. Res. Soc. Symp. Proc.* 1991, **227**, 211
11 Ree, M., Swanson, S. and Volksen, W. *ACS Polym. Prepr.* 1991, **32** (3), 308
12 Snyder, R. W. and Prada-Silva, G. Personal communication
13 Marquardt, D. W. *J. Soc. Ind. Appl. Math.* 1963, **11** (2), 431
14 Alexander, L. E. 'X-Ray Diffraction Methods in Polymer Science', Krieger, New York, 1979, p. 335
15 Scherrer, P. *Nachr. Gottinger Gesell.* 1918, **2**, 98
16 NCSASR. 'User Notes for 10-m SAXS Instrument', Oak Ridge National Laboratories, Oak Ridge, TN
17 Guinier, A. *Ann. Phys. (Paris)* 1939, **12**, 161
18 Alexander, L. E. 'X-Ray Diffraction Methods in Polymer Science', Krieger, New York, 1979, p. 312
19 Takahashi, N., Yoon, D. Y. and Parrish, W. *Macromolecules* 1984, **17**, 2583
20 Yoon, D. Y., Parrish, W., Depero, L. E. and Ree, M. *Mater. Res. Soc. Symp. Proc.* 1991, **227**, 387

21 Ree, M. unpublished results
22 Isoda, S., Shimada, H., Kochi, M. and Kambe, H. *J. Polym. Sci.: Polym. Phys. Edn* 1981, **19**, 1293
23 Russell, T. P. *J. Polym. Sci.: Polym. Phys. Edn* 1984, **22**, 1105
24 Russell, T. P. *Polym. Eng. Sci.* 1984, **24**, 345
25 Ree, M., Yoon, D. Y., Depero, L. E. and Parrish, W. *J. Polym. Sci.: Polym. Phys. Edn* submitted for publication
26 Song, H. H., Wu, D. Q., Chu, B., Satkowski, M., Ree, M., Stein, R. S. and Phillips, J. C. *Macromolecules* 1990, **23**, 2380
27 Kuhn, W. *Kolloid-Z.* 1936, **76**, 258
28 Kuhn, W. *Kolloid-Z.* 1939, **87**, 3
29 Hosemann, R. and Bagchi, S. N. 'Direct Analysis of Matter by Diffraction', North-Holland, Amsterdam, 1962, Ch. 18